Electronic transitions and genuine crystal-field parameters in copper metaborate CuB_2O_4

R. V. Pisarev,[1] A. M. Kalashnikova,[1] O. Schöps,[2] and L. N. Bezmaternykh[3]
[1]*Ioffe Physical-Technical Institute, Russian Academy of Sciences, 194021 St. Petersburg, Russia*
[2]*Institute of Physics, Dortmund Technical University, 44221 Dortmund, Germany*
[3]*Institute of Physics, Siberian Branch, Russian Academy of Sciences, 660036 Krasnoyarsk, Russia*
(Received 22 April 2011; revised manuscript received 17 June 2011; published 17 August 2011)

We present and analyze high-resolution α-, σ-, and π-polarized absorption spectra related to *d-d* electronic transitions in tetragonal metaborate CuB_2O_4 where copper Cu^{2+} ions occupy two crystallographically distinct 4*b* and 8*d* positions. The spectra are characterized by exceptionally rich fine structure in the spectral range of 1.4–2.4 eV. Six zero-phonon (ZP) lines originating from the electronic transitions within the Cu^{2+} ions in both positions are distinguished and identified. Symmetry analysis explains polarization properties of the ZP lines in the 8*d* positions but only partially explains them in the 4*b* positions. Reliable assignment of all six ZP lines to specific transitions allowed us to calculate genuine cubic *Dq* and tetragonal *Ds* and *Dt* crystal-field parameters for both positions. We show that the $(3r^2 - z^2)$ state, the energy of which is the measure of the Jahn-Teller splitting, is the highest 3*d* state for both types of Cu^{2+} ion positions. Using the obtained crystal-field parameters as the reference values, we estimated *Dq*, *Ds*, and *Dt* for several other cuprates with different Cu-O bond lengths. In particular, the 3*d* level splitting in La_2CuO_4, Nd_2CuO_4, $CuGeO_3$, $Sr_2CuO_2Cl_2$, and $Cu_3B_7O_{13}Cl$ was analyzed. Our estimates suggest that the Jahn-Teller splitting in some of these cuprates is larger than it was assumed previously.

DOI: 10.1103/PhysRevB.84.075160 PACS number(s): 71.70.Ch, 71.70.Ej, 78.40.Ha

I. INTRODUCTION

It has been known for decades that copper compounds display a wide variety of exotic behaviors. Copper ions of manifold valency may occupy crystallographic positions with different coordinations and geometries. Many complexes exist where copper ions enter 2, 4, 5, and 6 nearest-neighbors positions, which often are markedly distorted. This ability leads to rich variety of physical properties of copper compounds, in particular oxides, such as insulator-to-metal transitions, structural phase transitions, spin-Peierls transitions, and so on. Strong variations of magnetic, electric, and optical properties as a function of doping are frequently observed. The best known example is the transition of highly resistive magnetically ordered insulators into high-T_C superconductors. Papers on this and related topics are numerous and are reviewed in Refs. 1–3.

Copper metaborate CuB_2O_4 is known for quite a long time[4] but its crystal structure was identified[5] only in 1971 and refined later.[6] Quite recently it was found as a mineral named santarosaite.[7] Among the wide variety of copper compounds, CuB_2O_4 received a vivid attention only recently due to several interesting physical properties markedly different from those in other cuprates.[8–20] From the chemical point of view, this material is one of a few known examples where 12 copper Cu^{2+} ions of the same type occupy two crystallographically distinct positions in the unit cell. The complex crystal structure and large unit cell with magnetic Cu^{2+} ions in different positions lead to intricate magnetic structures and rich magnetic phase diagram with antiferromagnetic ordering below $T_N = 21$ K followed by several phase transitions at lower temperatures. Commensurate and incommensurate magnetic structures are observed as a result of intrasublattice and intersublattice mutual interactions. Along with interesting magnetic, acoustic, dielectric, and other properties, this material demonstrates a rich variety of linear and nonlinear optical properties. A couple of examples are magnetic-field-induced second-harmonic generation,[21,22] recently reported magnetic-field-induced chirality, and magneto-electric dichroic signals.[23] The latter report was followed by a conflicting discussion in which the main arguments inevitably involved analysis of the macroscopic crystal symmetry, magnetic symmetry and the microscopic nature of electronic transitions in copper metaborate.[24–26]

In this paper, we report a detailed study of *d-d* electronic transitions in CuB_2O_4. Polarized absorption spectra were studied at low temperature with high spectral resolution in the range of 1.4–2.4 eV. We identified all expected six zero-phonon (ZP) lines for Cu^{2+} ions in both crystallographic positions. The analysis is given in terms of the crystal-field theory[27,28] yielding the values of the cubic *Dq* and tetragonal *Ds* and *Dt* parameters in both copper positions calculated with high accuracy. Since these parameters are determined by equatorial and apical distances between copper ions and ligands, we were able to estimate the crystal-field parameters in some other copper compounds where Cu^{2+} ion occupies similar local positions. This analysis allowed us to calculate the Jahn-Taller splitting, the value of which is often a matter of debate in copper compounds. We argue that this value was significantly underestimated in several previous reports.

The paper is organized as follows. In Sec. II, we describe the local coordination of Cu^{2+} ions in CuB_2O_4 and some other related copper compounds. In Sec. III, we describe the details of measurements of the optical absorption spectra. Experimental results are presented in Sec. IV. Symmetry analysis of the observed absorption features in both crystallographic positions is given in Sec. V. Genuine crystal-field parameters of CuB_2O_4 are discussed in Sec. VI. In Sec. VII, we analyze

d-d transitions, crystal-field parameters, and the Jahn-Teller splitting in several other copper compounds.

II. CRYSTAL STRUCTURE OF CuB_2O_4

Copper metaborate CuB_2O_4 crystallizes in a noncentrosymmetric tetragonal structure with a point group symmetry $\bar{4}2m$ and the space group $I\bar{4}2d$ ($N^o 122$).[5,8,29] The unit cell contains 12 formula units. The structure consists of a strongly coupled network of BO_4 tetrahedra with cavities between them occupied by the copper ions. The 12 Cu^{2+} ions in the unit cell are distributed between the 4*b* and 8*d* positions. Cu^{2+} ions in the 4*b* positions are surrounded by four nearest-neighbor (NN) oxygen O^{2-} ions arranged in a planar-square coordination in such a way that the Cu^{2+} ions are displaced at 0.010 Å from the oxygen plane in the direction of the tetragonal optical axis, see Fig. 1(a). In this position, the four copper-oxygen bond lengths are 1.999 Å and the local symmetry of the Cu^{2+} ions is therefore S_4 ($\bar{4}$). In the 8*d* positions, Cu^{2+} ions are surrounded by four NN equatorial oxygen O^{2-} ions and the average copper-oxygen separation in the equatorial plane is 1.937 Å . Structural study[5] shows the presence of two other apical oxygen ions at an exceptionally long $Cu^{2+}(8d)$-O^{2-} distance of 3.069 Å, which form a strongly distorted octahedron [see Fig. 1(b)]. The local symmetry of the 8*d* positions is C_2 (2). We note that the local twofold y' axes for the Cu^{2+} (8*d*) ions coincide either with *x* or *y* crystallographic axis, while the local z' axes do not coincide with the orientation of the crystallographic *z* axis. These local symmetry properties of copper positions are important for our analysis of polarized absorption spectra.

In this paper, we also consider the splitting of $3d^9$ electronic states in some copper compounds where Cu^{2+} ions occupy positions similar to those in CuB_2O_4. As examples of copper compounds where Cu^{2+} ions have distorted octahedral coordination we consider La_2CuO_4,[30] $CuGeO_3$,[31] $Sr_2CuO_2Cl_2$,[32] and

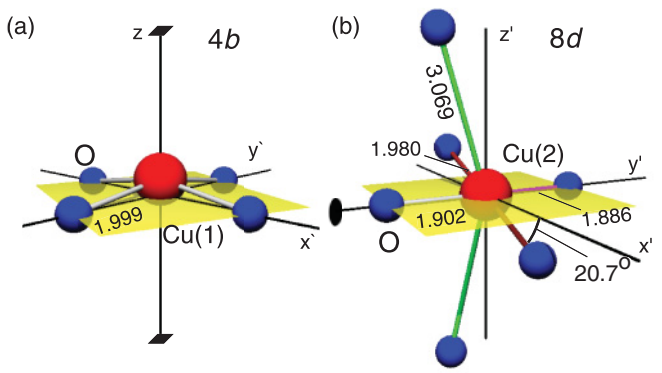

FIG. 1. (Color online) Schematic representation of the two crystallographic positions of Cu^{2+} ions in CuB_2O_4. (a) A planar-square complex CuO_4 with the S_4 ($\bar{4}$) local symmetry. The local *z* axis is parallel to the crystallographic symmetry axis $\bar{4}$. Displacement of the Cu^{2+} ion along the *z* axis by 0.010 Å is enhanced for the sake of clearness. (b) A distorted octahedron CuO_6 with the $C_2(2)$ local symmetry. The oxygen ions in the equatorial plane form a slightly distorted square unit which is almost confined with the (100) or (010) planes.[5,8] Numbers indicate the Cu^{2+}-O^{2-} bond lengths in Å. Similar colors represent the bonds of the same length.

TABLE I. Propagation direction and polarization of light in α-, σ-, and π-spectra in a uniaxial crystal with the optical axis parallel to the crystallographic *z* axis.[35]

Spectrum	**k** ($\hbar\omega$)	**E** ($\hbar\omega$)	**H** ($\hbar\omega$)
α (axial)	$\parallel z$	$\parallel x(y)$	$\parallel y(x)$
σ	$\parallel y(x)$	$\parallel x(y)$	$\parallel z$
π	$\parallel y(x)$	$\parallel z$	$\parallel x(y)$

$Cu_3B_7O_{13}Cl$.[33] Thus Cu^{2+} ions in $CuGeO_3$ and $Cu_3B_7O_{13}Cl$ occupy cavities formed by networks of GeO_4 and BO_4 tetrahedra, respectively. Distortions of the CuL_6 octahedra (L stands for a ligand) in these compounds are smaller than in CuB_2O_4. Cu^{2+} ions in Nd_2CuO_4 occupy planar-square positions,[34] which are analogous to 4*b* positions in CuB_2O_4, see Fig. 1(a).

III. EXPERIMENTAL DETAILS

Absorption measurements were performed using two types of spectrometers. Broad range absorption measurements were performed on a Cary 2300 spectrophotometer equipped with a sample held in a closed-cycle helium cryostat. High-resolution-optical-absorption spectra were measured with a use of a Spex 0.85 m double monochromator equipped with a cooled charge-coupled device for the detection of the transmitted light. During all measurements the monochromator slits were kept as narrow as 10 μm and spectral resolution was estimated to be better than 0.1 meV in the visible range. Samples were placed in an optical helium cryostat. Three types of absorption spectra were measured with polarization properties listed in Table I.

Large single crystals of good optical quality were grown by a Kyropulos method from the melt of oxides B_2O_3, CuO, Li_2O, and MoO_3.[14] Plane-parallel polished plates of (100) and (001) orientation were prepared from x-ray oriented single-crystal boules. Typical thicknesses of the samples were 100 μm and below. The refractive index was derived from reflectance measurements from an undetermined as-grown face of a single crystal and was found to be of $n = 1.75$–1.77 (at 2.0 eV) and $n = 1.78$–1.80 (at 3.0 eV). A close value $n = 1.75$ was recently reported for a mineral santarosaite.[7]

IV. ABSORPTION SPECTRA INDUCED BY *d-d* CRYSTAL-FIELD TRANSITIONS

A. Absorption spectra of CuB_2O_4 below the fundamental band gap

Figure 2 shows the π-spectrum of the copper metaborate measured at a relatively high temperature of $T \simeq 40$ K in a broad range of photon energies of 1.3–4.2 eV. Below 1.35 eV, CuB_2O_4 is transparent. A complex absorption band is seen in the range of 1.35–2.5 eV. Above 2.5 eV, CuB_2O_4 becomes transparent up to 3.8 eV where the fundamental absorption due to charge-transfer (CT) transitions begins. Residual absorption in CuB_2O_4 within the transparency window 2.5–3.8 eV seen in Fig. 2 is due to reflection losses and absorption tails of the complex 2 eV and the fundamental absorption bands. This window defines a dark blue color of CuB_2O_4 in thick plates of

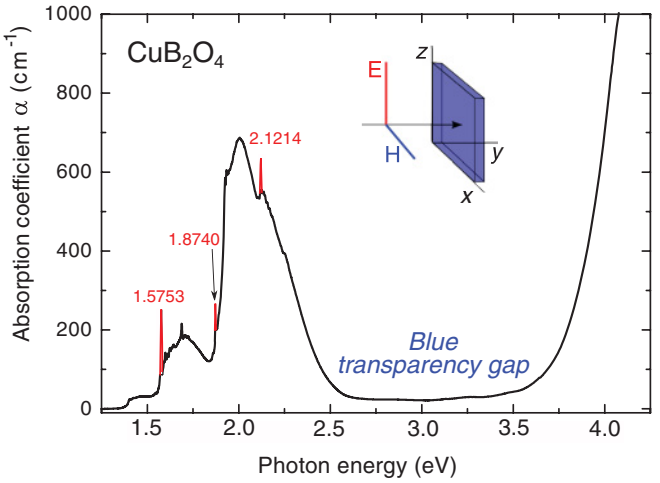

FIG. 2. (Color online) Absorption π-spectrum of CuB_2O_4 below the fundamental absorption edge at $T \simeq 40$ K. No correction for reflection losses was taken, which explains residual absorption in the blue transparency window of 2.5–3.7 eV. Numbers indicate photon energies of the ZP lines. Inset show the light polarization and propagation directions for the π-spectrum (see also Table I).

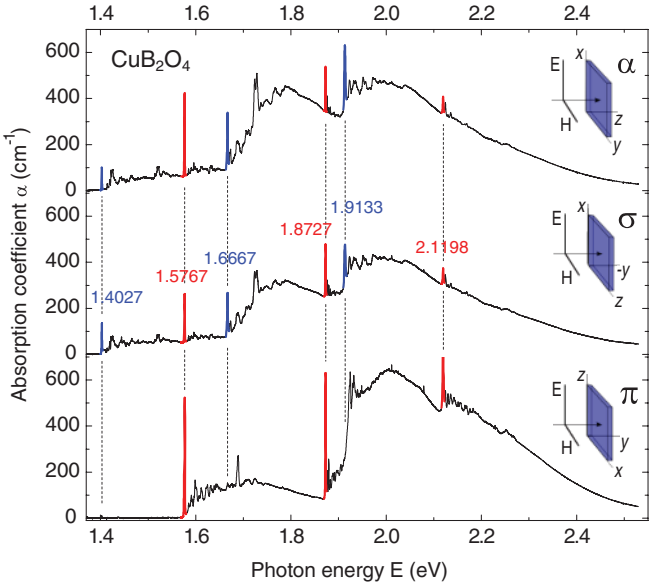

FIG. 3. (Color online) α-, σ- and π-absorption spectra of CuB_2O_4 in the range of d-d transitions measured at $T = 5$ K. Numbers are the positions of ZP lines in eV. Blue peaks are the lines appearing only in the α- and σ-spectra. Red peaks are the zero-phonon lines appearing in all three types of spectra. Insets show the light polarization and propagation directions for the corresponding spectra (see also Table I).

about 1 mm and thicker, and a pale blue color of thin plates with a thickness about 0.1 mm and thinner. We note that relatively low absorption of the d-d bands and high transparency in the visible range is observed in other borates, for example, in green $3d^5$-iron borates $FeBO_3$ and $GdFe_3(BO_4)_3$,[36,37] with a noticeable exception of Fe_3BO_6 with high concentration of Fe^{3+} ions.[38]

With respect to the observed absorption spectra, it is appropriate to discuss in brief optical properties of insulating cuprates, in particular, their properties in the visible spectral range. From this point of view, they can be divided roughly into two groups of opaque and transparent cuprates. Transparent cuprates may be regarded as predominantly ionic compounds where the CT transitions are situated in the spectral range above the relatively weak d-d crystal-field transitions. Evidently, copper metaborate belongs to this group of cuprates. Other examples of the ionic copper compounds are, first of all, highly ionic fluorides such as K_2CuF_4[39–41] and $KCuF_3$.[42] They are characterized by stronger ionicity in comparison to oxides and, consequently, a broader spectral range of optical transparency, which is disturbed, in part, by relatively weak intraionic d-d electronic transitions. There are also several examples of transparent copper oxides with high concentration of copper ions. We restrict ourselves in this paper to two compounds. The optical properties of $CuGeO_3$[43–45] have a lot in common with those of the copper metaborate. Another material we discuss is a copper boracite oxychloride, $Cu_3B_7O_{13}Cl$. Absorption spectra of this material are characterized by broad complex d-d bands at 1.0–1.5 eV with a transparency window from approximately 2 to 3 eV.[46]

Opaque cuprates form another broad group and belong often to strongly correlated materials. The optical band gap in these materials is governed by intensive CT transitions, which are situated at a photon energy lower than the weak d-d crystal field transitions.[47] The reason for such a low energy shift of the CT transitions is strong covalency in this type of cuprates. As a rule, weaker d-d transitions in such materials are hard to distinguish in optical measurements. Therefore, the x-ray methods, in particular resonance inelastic x-ray scattering (RIXS), are used for this purpose.[48–51] As examples of opaque cuprates, we discuss in Sec. VII rare-earth cuprates La_2CuO_4, Nd_2CuO_4,[1,3,52] and oxychloride $Sr_2CuO_2Cl_2$.[32,48,53] Many examples of optical absorption spectra of inorganic copper compounds and minerals can be found in monographs.[27,28]

B. Polarized absorption spectra of CuB_2O_4 in the range of the d-d transitions

Figure 3 shows α-, σ-, and π-polarized absorption spectra of CuB_2O_4 in the range of 1.4–2.5 eV, registered at low temperature $T = 5$ K with high spectral resolution. Insets in these plots show the sample orientation and the polarization of the incoming light $\mathbf{E}(\hbar\omega)$, $\mathbf{H}(\hbar\omega)$ for each spectrum. The spectral structure is unusually rich. It allows us, first of all, to distinguish six narrow sharp absorption features followed by broad sidebands with well pronounced fine structure, as shown in Fig. 3. These six lines differ essentially from other lines in the spectra. First, they appear to be the narrowest. Second, out of all rich absorption-lines structure only they contribute to the spectra of the second harmonic signal, as was reported previously in Ref. 21. Therefore, we can assign these six sharp features to zero-phonon lines, which correspond to localized d-d electronic transitions in the Cu^{2+} ions. The main parameters of these six lines such as position, full width at half maximum (FWHM), and their polarization properties are summarized in Table II.

We would like to emphasize that the d-d absorption spectra of CuB_2O_4 are quite unique. Thus each ZP line is followed

TABLE II. Positions, FWHM, polarization properties of the six ZP lines in the absorption spectra of CuB_2O_4 (Fig. 3), and their assignment to transitions in 4*b* and 8*d* Cu^{2+} ion positions (see discussion in the text).

Energy (eV)	FWHM (eV)	Spectrum			Cu^{2+} position
1.4027	1.1×10^{-3}	α	σ		4*b*
1.5767	1.1×10^{-3}	α	σ	π	8*d*
1.6667	1.8×10^{-3}	α	σ		4*b*
1.8727	1.1×10^{-3}	α	σ	π	8*d*
1.9133	4.0×10^{-3}	α	σ		4*b*
2.1198	2.4×10^{-3}	α	σ	π	8*d*

by multiple phonon sidebands. As an example, in Fig. 4 we show the ZP line at 1.4027 eV followed by multiple sideband structure where up to 70 features can be distinguished. For each of the six ZP lines, the electron-phonon structure is very specific, but its detailed analysis is outside the scope of the present paper. We note that some pronounced spectral features, e.g., the ones at photon energies 1.689 and 1.7238 eV, are considerably broader then the lines which we assign to the ZP *d-d* transitions. Therefore, those features must be assigned to phonon-assisted sidebands.

Within the numerous data on copper compounds no resembling spectra could be found. To confirm this conclusion let us cite several examples. First of all, in CuB_2O_4 only one *d-d* transition at 1.9 eV was resolved so far using the RIXS technique.[13] In highly ionic fluorides, the fine structure is usually better resolved than in oxides. In fact, phonon-assisted

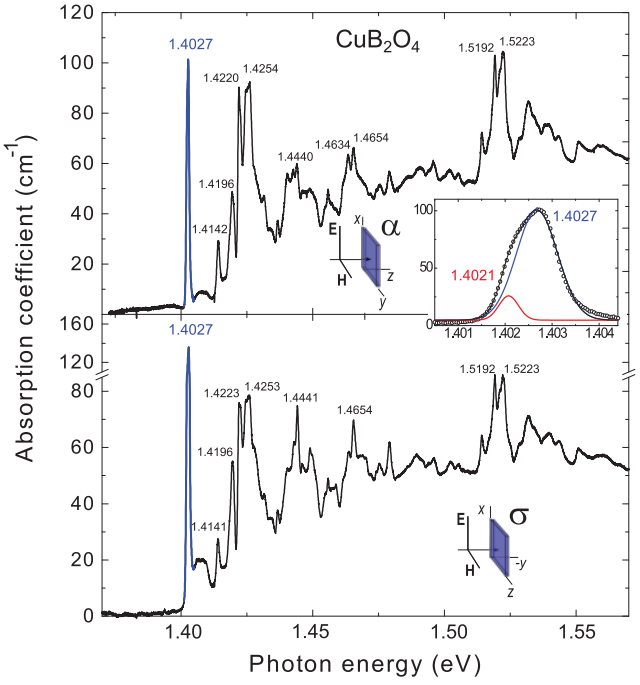

FIG. 4. (Color online) (a) α- and (b) σ-absorption spectra of CuB_2O_4 at $T = 5$ K in the range of the first ZP line at 1.4027 eV. Up to 70 phonon-assisted sidebands of this ZP line can be distinguished. Several well-resolved sidebands are marked. Inset shows the first ZP line in the α-spectrum and its decomposition into two Lorentzians.

electronic transitions were observed in fluorides K_2CuF_4 and $KCuF_3$.[39–42] However, in contrast to CuB_2O_4, only a single ZP line was detected in K_2CuF_4[41] and two ZP lines in $KCuF_3$.[42] Another example is $CuGeO_3$, the optical absorption of which is characterized by a broad complex band, which in its rough features is very similar to that of CuB_2O_4 shown in Fig. 2. Again, no fine structure but only three broad overlapping bands were observed in polarized spectra of $CuGeO_3$ at low temperature.[43,44] Subsequent publication showed that only a single ZP line can be detected in $CuGeO_3$ at 1.47 eV.[45] The width of 10 meV of this line is much broader than in CuB_2O_4 (see Table II). We add that no fine structure was ever observed in highly correlated opaque cuprates.

V. SYMMETRY ANALYSIS OF THE ELECTRONIC STRUCTURE OF Cu^{2+} IONS IN 4*b* AND 8*d* POSITIONS

Comparison of the polarization properties of the six observed ZP lines (see Table II) allow us to separate them into two sets. The first set involves the lines at 1.4027, 1.6667, and 1.9132 eV, which are observed only in α and σ spectra when the electric field of the light wave is perpendicular to the *z* crystallographic axis. The second set consists of three lines at 1.5766, 1.8726, and 2.1197 eV, which are observed in all three types of spectra, as Fig. 3 and Table II show.

In general case of Cu^{2+} compounds, one expects the presence of four transitions, which contribute to the *d-d* absorption spectra. Their energy, selection rules, and degeneracy are dictated by the symmetry and the crystal field of the local environment. Since in copper metaborate there are two distinct positions for the Cu^{2+} ion, we may conclude that the observed two sets of ZP lines correspond to the *d-d* transitions in these distinct copper ions. For further analysis, we consider the symmetry properties of the 4*b* and 8*d* crystallographic positions.

First of all, transitions between *d-d* states are parity forbidden in the electric-dipole (ED) approximation but may be allowed as magnetic-dipole (MD) transitions. For example, ZP lines in K_2CuF_4 and $KCuF_3$, where copper ions have an octahedral coordination, were treated as MD transitions.[39–42] However, the ED *d-d* transitions may become allowed if the local coordination of the Cu^{2+} sites lacks the inversion symmetry.[54] That is just the case in CuB_2O_4 where the 4*b* and 8*d* sites have the local symmetry $\bar{4}$ and 2, respectively (see Sec. II). The splitting of the 3*d* states of Cu^{2+} ion in these two sites is shown in Fig. 5.

We start from the distorted octahedron CuO_6 [see Fig. 1(b)], the energy levels for which are given in Fig. 5(b). The order of the excited levels will be discussed separately in the following section. As can be seen in Fig. 5(b), all *d-d* transitions are allowed in both ED and MD approximations, which is a natural consequence of the low symmetry of the distorted octahedron with broken space inversion. As the local axes of the CuO_6 octahedron do not coincide with the crystallographic axes *x*, *y*, and *z*, these transitions can be expected to be observed in all three types of polarized absorption spectra. Therefore, the set of the three ZP lines observed in all three spectra in Fig. 3 originates from the *d-d* transitions in Cu^{2+} ion occupying 8*d* sites. As ED transitions are typically stronger than MD transitions, we assign these three ZP lines to the *d-d*

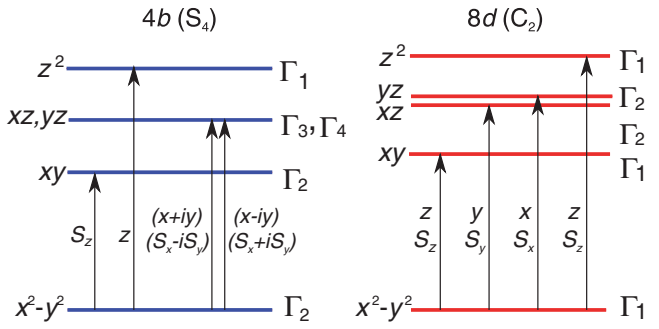

FIG. 5. (Color online) Schematic representation of the energy levels of the Cu^{2+} ions in CuB_2O_4 in (a) a planar-square complex CuO_4 with the local symmetry S_4 and (b) a distorted octahedron CuO_6 with the local symmetry C_2. Vertical arrows show symmetry allowed electric- and magnetic-dipole transitions. Notations are according to Ref. 55. Note that instead of the $3d^9$ scheme, we show the energy levels for a single hole.

of the ED nature in CuO_6 complex with symmetry C_2. The electric-dipole nature of these transitions was also confirmed in experiments with second harmonic generation.[21,22] We note that the splitting between the (xz) and (yz) levels required by the symmetry of the $8d$ position [see Fig. 5(b) is not observed in the experimental spectra, which indicates that the splitting is smaller than the width of the ZP line at 1.8727 eV.

The other three ZP lines vanishing in the π-spectra originate, therefore, from the d-d transitions in the Cu^{2+} ion occupying the $4b$ positions. These polarization properties clearly indicate the ED nature of the transitions, which, moreover, was confirmed in the experiments on the second harmonic generation.[21,22] The diagram for the d-d transitions, shown in Fig. 5(a), however, contradicts partly to the observed polarization properties of the three ZP lines. The symmetry of the $4b$ position predicts a more complicated picture with the first transition being of the MD nature. This controversy indicates that the symmetry of the CuO_4 complex is in fact lower than S_4, which could lift some of the restrictions and make all three transitions allowed in the ED approximation. For example, symmetry may become lower due to spin ordering at $T_N = 21$ K and several magnetic phase transitions observed in CuB_2O_4 below T_N.

VI. GENUINE CRYSTAL-FIELD PARAMETERS IN CuB_2O_4

In the previous section we analyzed symmetry restrictions on the selection rules and polarization properties of the electronic transitions in the two types of Cu^{2+} sites. Now we analyze the splitting of the $3d$ states in terms of the D_{4h} point group. The choice of this group is justified because tetragonal crystal-field distortions play the dominant role in the local environment of Cu^{2+} ion in both $8d$ and $4b$ positions. A small orthorhombic contribution may be present in the $8d$ position, which would induce a splitting between the (xz) and (yz) states. Absence of any noticeable splitting of these states in the experimental spectra justify the applicability of the tetragonal D_{4h} group. Further deviation of the Cu^{2+} environment from this point group yields, first of all, the specific selection rules for the d-d transitions, but does not affect significantly their energies.

For describing the problem of energy splitting we apply results of the crystal-field theory, which takes into account, along with the cubic-crystal-field parameter Dq, two tetragonal parameters Ds and Dt.[27,28] In the crystal-field theory for a metal Me-ligands L complex MeL_N of the point group D_{4h}, these parameters are defined as[27]

$$Dq = \frac{1}{6} Ze^2 \frac{\bar{r}^4}{d_e^5},$$
$$Ds = \frac{2}{7} Ze^2 \left(\frac{\bar{r}^2}{d_e^3} - \frac{\bar{r}^2}{d_a^3} \right), \quad (1)$$
$$Dt = \frac{2}{21} Ze^2 \left(\frac{\bar{r}^4}{d_e^5} - \frac{\bar{r}^4}{d_a^5} \right),$$

where Z is the ligand charge, e is the electron charge, and $\bar{r}$ is the mean value of the electron distribution radii in the metal ion. The inverse fifth-power dependency of the cubic crystal-field splitting $10Dq$ on the equatorial metal-ligand distance d_e is of fundamental importance. Parameters Ds and Dt arise due to the compression/elongation of the octahedron along the fourfold symmetry axis. That is the difference between the equatorial d_e and apical d_a metal-ligand distances, which is the source of the tetragonal splitting. In particular, $d_a = \infty$ in a planar-square MeL_4 complex.

The free Cu^{2+} ion has the electronic structure $3d^9$ or the hole structure $3d^1$, which are split by the cubic crystal field into t_{2g} and e_g orbitals. These orbitals are further split by noncubic distortions. The relevant matrix elements for the four electronic states of a single d hole in tetragonal crystal field of the point group D_{4h} are given in Table III. Notations $\Gamma_3^+(B_{1g})$, $\Gamma_1^+(A_{1g})$, $\Gamma_4^+(B_{2g})$, and $\Gamma_5^+(E_g)$ are given according to Refs. 55 and 27.

The first important conclusion from this analysis follows immediately for the sequence of the $3d$ states in the planar-square $4b$ positions. Crystal-field theory strictly defines the sequence of the states,[27,28] which is shown in Fig. 6(a). The ground state is the $\Gamma_3^+(x^2 - y^2)$ state and the excited states are, as the excitation energy grows, $\Gamma_4^+(xy)$, $\Gamma_5^+(xz,\ yz)$, and the

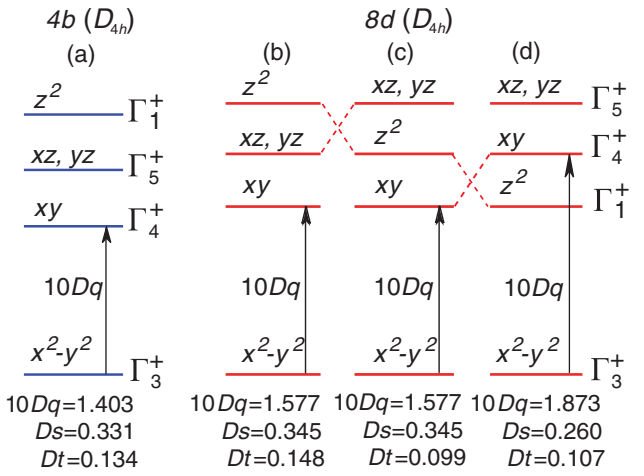

FIG. 6. (Color online) Splitting of the $3d$ states of Cu^{2+} ions for the D_{4h} symmetry in the $4b$ positions (a) and in $8d$ positions (b)–(d) with different choice of crystal-field parameters.

TABLE III. Matrix elements for the five states of a single d hole in a tetragonal crystal field of the point group (PG) D_{4h} according to Refs. 55 and 27.

Electronic state	Notation PG D_{4h}	Matrix elements in terms of Dq, Ds, and Dt
x^2-y^2	Γ_3^+	$6Dq+2Ds-Dt$
$3r^2-z^2$	Γ_1^+	$6Dq-2Ds-6Dt$
xy	Γ_4^+	$-4Dq+2Ds-Dt$
xz, yz	Γ_5^+	$-4Dq-Ds+4Dt$

highest state is $\Gamma_1^+(3r^2-z^2)$. The positions of the three ZP lines are available from our experimental data in CuB_2O_4 and this finding provides a unique opportunity for calculating all three genuine tetragonal crystal-field parameters. By saying "genuine" we mean that parameters could be calculated on the basis of exact positions of pure electronic states, but not from the positions of maxima of broad absorption bands as it is usually done in numerous optical studies or in recent resonant inelastic x-ray scattering (RIXS) studies.[48,56] Calculated genuine crystal-field parameters Dq, Ds, and Dt for the $4b$ Cu^{2+} position are listed in Fig. 6(a).

The second conclusion is that the energy difference between the ground state $\Gamma_3^+(x^2-y^2)$ and the first excited state $\Gamma_4^+(xy)$ is exactly $10Dq$. Now, using matrix elements in Table III, one can easily calculate the tetragonal parameters Ds and Dt for the $4b$ positions. It is worth reminding that a planar-square oxygen coordination of Cu^{2+} ions occurs in many cuprates, e.g., in the T'-type cuprates such as Nd_2CuO_4.[34] From this purely symmetry-based analysis it follows that the energy of the $3d$ states in compounds with Cu^{2+} ions in the planar-square positions must follow the same sequence as in the $4b$ positions in CuB_2O_4.

Establishing the sequence of states for the $8d$ sites is not so straightforward as in the case of the $4b$ sites. In fact, in ideal octahedral positions, the $\Gamma_3^+(x^2-y^2)$ and $\Gamma_1^+(3r^2-z^2)$ states are degenerate. In most cases this degeneracy is lifted as a consequence of the Jahn-Teller effect. In a compressed octahedron, the $(3r^2-z^2)$ state becomes the ground state. To date, there are only a few examples of Cu^{2+} compounds with a compressed geometry.

By contrast, there are many examples of Cu^{2+} ions in elongated octahedra where the ground state is the (x^2-y^2) state. Obviously the magnitude of the Jahn-Teller splitting depends on the degree of distortions of ideal octahedron. Therefore, proper positioning of the $(3r^2-z^2)$ state in measured or calculated spectra is a challenging task and often leads to a controversy. Rare-earth cuprates R_2CuO_4 are well-known examples of the copper compounds with elongated octahedral positions.[1–3] In La_2CuO_4, the elongated octahedron is characterized by four equatorial Cu-O bonds as long as 1.8971 Å and two apical bonds of 2.4289 Å.[30] The position of the Γ_1^+ $(3r^2-z^2)$ state in La_2CuO_4 is supposed to be at ~0.5–2 eV,[57–60] however, there is no experimental evidence of true energy of this level. Another example is K_2CuF_4. In a number of early works, the $(3r^2-z^2)$ state was assigned to a spectral feature at 0.12 eV.[39,40] However, a later paper presented more arguments in favor of the $(3r^2-z^2)$ state being associated with a broad absorption band at 1.033 eV.[41] A similar feature with a maximum absorption at 1.02 eV was reported recently in the spectra of $KCuF_3$.[42] Similar controversy exists regarding the $(3r^2-z^2)$ level position in oxychloride $Sr_2CuO_2Cl_2$.[48,53,61]

Figures 6(b)–6(d) shows three different alternatives of the electronic structure in the elongated octahedral site $8d$. Figures 6(a) and 6(b) show the same sequences of states for both $4b$ and $8d$ sites when the $(3r^2-z^2)$ state takes the highest energy. Figure 6(d) shows the sequence when this state has the lowest excitation energy. And finally, Fig. 6(c) shows the sequence when the $(3r^2-z^2)$ state lies between the (xy) and (xz, yz) states. For example, the sequence in Fig. 6(d) corresponds to the case of copper fluorides K_2CuF_4 and $KCuF_3$ discussed above.[41,42] The particular values of the crystal-field parameters Dq, Ds, and Dt can be calculated using the matrix elements in Table III for each sequence of states, as shown in Fig. 6.

Simple crystal-field calculations using Eq. (1) allow us to disregard the sequence (d) in Fig. 6 for the case of the $8d$ sites. In fact, the theory states that the cubic parameter Dq in octahedral sites is defined by four equatorial oxygens similar to the planar square positions $4b$.[27] Using Eq. (1) and the Cu^{2+}-O^{2-} bond lengths in both types of sites, we calculated $Dq(8d)$ taking $Dq(4b) = 0.1403$ eV as a reference. The obtained value of $Dq(8d) = 0.1634$ eV is only 4% higher than the $Dq = 0.1577$ eV value obtained from the experimental data for the sequences of states (b) and (c) in Fig. 6. By contrast, for the sequence (d) the parameter $Dq = 0.1873$ eV is about 34% higher than the estimated value $Dq(8d) = 0.1634$ eV. No cause can be found for such a strong increase of Dq and, therefore, the sequence (d) can be disregarded.

Comparing parameters in Figs. 6(b) and 6(c), one can see that they differ only by the value of the Dt parameter. The sequence (b) seems to be a more reasonable choice for the realistic electronic structure. When comparing the $8d$ and $4b$ sites, only in this case we have systematic increase of all three parameters Dq, Ds, and Dt by 12, 11, and 10%, respectively (see Table IV). This conclusion is supported by the structural data of CuB_2O_4. It was stated that both types of Cu^{2+} positions, despite their symmetry differences, are very similar.[5] In fact, in the first approximation all positions of Cu^{2+} ions can be considered as planar square. Existing symmetry differences such as orientation of local axes with respect to the crystallographic axes are revealed in the polarization properties of the spectra of Cu^{2+} ions in the $4b$ and $8d$ positions, as discussed in Sec. V. Therefore, based on this analysis we can identify the order of the $3d$ energy levels and define with confidence all genuine crystal-field parameters for $8d$ and $4b$ positions of Cu^{2+} ion, which are listed in Table IV.

VII. ESTIMATES OF THE CRYSTAL-FIELD PARAMETERS IN SOME COPPER COMPOUNDS

As we mentioned above, CuB_2O_4 is a unique example of a copper compound that possesses unexpectedly well resolved absorption spectra in the range of the d-d transitions. After calculating the genuine crystal-field parameters for copper metaborate, we can use them for estimating these parameters in other compounds, in which Cu^{2+} ions occupy similar or

analogous crystallographic positions. Here, we use the fact that the copper ion coordination and the Cu-O bond lengths are the decisive factors in forming the energy spectra.[27] The analysis of the optical Raman spectra of some copper oxides reported in Refs. 62 and 49 has proven the validity of such an approach. The systematic changes in the *d-d* spectra due to the ratio of apical-to-equatorial bond lengths were studied *ab initio* in some copper compounds.[63]

In Table V, we summarize the data on Cu^{2+}-O^{2-} bond lengths in CuB_2O_4, $CuGeO_3$, rare-earth cuprates La_2CuO_4 and Nd_2CuO_4, oxychlorides $Sr_2CuO_2Cl_2$, and $Cu_3B_7O_{13}Cl$. These compounds can be, for the sake of convenience, divided into two groups depending on the planar-square or (distorted) octahedral positions occupied by the Cu^{2+} ion. Thus Cu^{2+} ions enter planar-square positions CuO_4 in Nd_2CuO_4, and tetragonally distorted octahedral positions CuO_6 in La_2CuO_4 and $CuGeO_3$. In $Sr_2CuO_2Cl_2$, Cu^{2+} ions occupy positions CuO_4Cl_2 with D_{4h} symmetry with four O^{2-} ions in the equatorial plane and two apical Cl^- ions.[32] In boracites, Cu^{2+} ions occupy positions CuO_4Cl_2 with the S_4 ($\bar{4}$) symmetry[33,64] similar to 4*b* positions in CuB_2O_4. The nearest Cu^{2+} neighbors are four O^{2-} ions in the equatorial plane and two apical Cl^- ions.

Here, we use the crystal-field parameters *Dq*, *Ds*, and *Dt* in CuB_2O_4 for calculating these parameters in other compounds taking into account the relevant bond lengths according to Eq. (1). The value of *Dq* according to the crystal-field theory is defined by four equatorial bond lengths d_e and corresponds to the $(x^2 - y^2) \rightarrow (xy)$ transition. Table V shows that $10Dq$ changes from the smallest value 1.403 eV in square planar positions in CuB_2O_4 up to 1.758 eV in La_2CuO_4.

Numerous data on the value of splitting between the $(x^2 - y^2)$ and (xy) states can be found in literature, including both experimental and theoretical works. In Table V, we provide experimental data adopted from literature along with the values obtained from our calculations. The energies of the $(x^2 - y^2) \rightarrow (xy)$ transition for La_2CuO_4 (1.74 eV) and Nd_2CuO_4 (∼1.5 eV) were obtained from the large-shift optical Raman spectra.[49] In La_2CuO_4, a peak in the midinfrared electroreflectance spectrum at 1.4 eV was assigned to $(x^2 - y^2) \rightarrow (xy)$ transition.[50]

In $CuGeO_3$, the only ZP line at 1.470 eV was observed in the optical spectra and assigned to the transition $(x^2 - y^2) \rightarrow (xy)$.[45] In earlier work, a complex broad absorption band in the region between 1.4 and 2.3 eV was reported and assigned to the *d-d* transitions in the Cu^{2+} ions.[43] Three bands centered at 1.55, 1.7, and 1.9 eV could be distinguished within this absorption band. Analogous features were reported in the absorption spectra of $CuGeO_3$, but in contrast to the previous paper, they were assigned to transitions between the critical points in the valence and conduction bands.[44] However, this assignment does not seem to be sufficiently justified.

In $Sr_2CuO_2Cl_2$, RIXS experiments gave a value of 1.35 eV for the $(x^2 - y^2) \rightarrow (xy)$ transition.[48] A complex absorption band in boracite $Cu_3B_7O_{13}Cl$ at photon energy of ∼1.24 eV was observed and assigned to the $(x^2 - y^2) \rightarrow (xy)$ transitions.[46] Taking into account the considerable simplicity of our model, there is a firm agreement between our estimates for the $(x^2 - y^2)$-(xy) splitting in the considered cuprates and the data available in literature.

One can see that the *Ds* and *Dt* parameters calculated in our model vary weakly from one compound to another with an exception of La_2CuO_4 characterized by the smallest value of d_a/d_e and, consequently, by the smallest values of *Ds* and *Dt*. We note that for calculating *Ds* and *Dt* parameters in $Sr_2CuO_2Cl_2$ and $Cu_3B_7O_{13}Cl$ the charge *Z* of the apical ligands in Eq. (1) had to be reduced by a factor of two in order to account for the the substitution of oxygen O^{2-} ions by chlorine Cl^- apical ions.

Having calculated all three crystal-field parameters we were able to estimate the energies of the (xz, yz) and $(3r^2 - z^2)$ levels of the Cu^{2+} ion in octahedral and planar-square coordination using the expressions from Table III. The results are summarized in Table V. Comparison of the obtained values with those from experimental studies is difficult, since there is a very limited number of experiments where these transitions could be resolved.

There are, however, a few experimental studies, where the directly observed features in optical or x-ray spectra were ascribed to $(x^2 - y^2) \rightarrow (xz, yz)$ transition. In La_2CuO_4, the $(x^2 - y^2) \rightarrow (xz, yz)$ transition was detected at 1.6 eV in the midinfrared electroreflectance spectra.[50] A feature in RIXS spectra of La_2CuO_4 observed at ∼1.8 eV was ascribed to a *d-d* transition, without specifying its symmetry.[56] A recent RIXS study of Nd_2CuO_4 allowed the identification of the $x^2 - y^2 \rightarrow xz, yz$ in this cuprate at the photon energy of 1.65 eV.[51]

In $Sr_2CuO_2Cl_2$, a feature corresponding to the transition $(x^2 - y^2) \rightarrow (xz, yz)$ was observed in RIXS spectra.[48] In the absorption spectrum of $Cu_3B_7O_{13}Cl$, the band at 1.48 eV was assigned to the (xz, yz) transition. Again, these experimental data are in good agreement with the values calculated here.

Figure 7 shows how the energies of all four *d-d* transitions vary in the copper compounds with octahedral Cu^{2+} coordination as a function of the octahedron elongation. As one can see, our calculations predict that in all considered copper compounds the level $(3r^2 - z^2)$ appears to have the highest energy. The only exception is La_2CuO_4 where the Cu-O equatorial bond length $l_e = 1.8971$ Å is the shortest among the discussed cuprates.[30] As a reference, we have also calculated the evolution of the energies of these levels in a octahedral complex CuO_6 with equatorial Cu-O bond length $d_e = 1.962$ Å, which is the average over d_e in all considered CuL_6 clusters. The deviation of the results for the real CuL_6 clusters from these dependencies is a natural consequence of the fact that they all have different bond lengths d_e. However, the calculated dependence gives a clear idea of how the position of the $(3r^2 - z^2)$ depends on the octahedron elongation d_a/d_e. As one can see from Fig. 7, in such a cluster the level $(3r^2 - z^2)$ becomes higher than the level (xz, yz) when the elongation of

TABLE IV. Crystal-field parameters *Dq, Ds*, and *Dt* (in eV) for two positions of the Cu^{2+} ion calculated from the positions of ZP lines in the absorption spectra given in Table II for the electronic-states order shown in Fig. 6(b).

Cu^{2+} ion position	*Dq*	*Ds*	*Dt*
4*b* (planar-square CuO_4)	0.1403	0.311	0.134
8*d* (elongated octahedron CuO_6)	0.1577	0.345	0.147
Ratio of parameters $8d/4b$	1.124	1.109	1.097

TABLE V. Cu^{2+}-O^{2-} bond lengths, calculated crystal-field parameters Dq, Ds, and Dt and the Jahn-Teller splitting E_{JT} in some copper compounds with octahedral and planar square Cu^{2+} coordinations. Also presented are some data for energy levels adopted from experimental results, reported elsewhere (in italic font).

Compound	Ideal octahedron	La_2CuO_4[a]	$CuGeO_3$[b]	$Sr_2CuO_2Cl_2$[c]	$Cu_3B_7O_{13}Cl$[d]	CuB_2O_4[e] (8*d*)	Nd_2CuO_4[f]	CuB_2O_4[e] (4*b*)
Coordination	octahedron						planar-square	
		CuO_6		CuO_4Cl_2		CuO_6	CuO_4	
Equatorial bond d_e (Å)	d_e	1.8971	1.9326	1.986	2.023	1.937[g]	1.971	1.999
Apical bond d_a (Å)	$d_a = d_e$	2.4289	2.7549	2.859	3.025	3.069	∞	∞
Ratio d_a/d_e	1.00	1.280	1.425	1.440	1.495	1.584	∞	∞
$10Dq$ (eV)	$10Dq$	1.735	1.581	1.391	1.258	1.577[h]	1.505	1.403[h]
Ds (eV)	0	0.255	0.303	0.355	0.345	0.345[h]	0.324	0.311[h]
Dt (eV)	0	0.125	0.137	0.129	0.125	0.147[h]	0.144	0.134[h]
E_{xy} (eV)	$10Dq$	1.74	1.58	1.39	1.26	1.577[i]	1.51	1.403[i]
		1.7[j], *1.4*[k]	*1.470*[l]	*1.35*[m], *1.5*[n]	*1.24*[o]		*1.5*[j]	
$E_{xz,yz}$ (eV)	$10Dq$	1.84	1.83	1.78	1.69	1.873[i]	1.76	1.667[i]
		1.6[k]		*1.7*[m]	*1.48*[o]		*1.65*[p]	
$E_{3r^2-z^2}$=E_{JT} (eV)	0	1.42	1.90	2.07	2.01	2.12[i]	2.02	1.913[i]
				0.4[n]				*1.9*[q]

[a]Cu^{2+}-O^{2-} bond lengths are according to Ref. 30.
[b]Cu^{2+}-O^{2-} bond lengths are according to Ref. 31.
[c]Cu^{2+}-O^{2-} and Cu^{2+}-Cl^{-} bond lengths are according to Ref. 32.
[d]There are no data on bond lengths in $Cu_3B_7O_{13}Cl$ available. Therefore, Cu^{2+}-O^{2-} and Cu^{2+}-Cl^{-} bond lengths in $Mg_3B_7O_{13}Cl$ [33] are given instead. These bond lengths are expected to be close to those in the boracite, as the ionic radii of Cu^{2+} and Mg^{2+} with coordination VI are very close.
[e]Cu^{2+}-O^{2-} bond lengths are according to Ref. 5.
[f]Cu^{2+}-O^{2-} bond lengths are according to Ref. 34.
[g]Average bond length.
[h]Value calculated from the absorption spectra in Fig. 3.
[i]Figure 3.
[j]Reference 49.
[k]Reference 50.
[l]Reference 45.
[m]Reference 48.
[n]Reference 61.
[o]Reference 46.
[p]Reference 51.
[q]This value determined from the RIXS spectra[13] was assigned to one of the *d*-*d* transitions.

the octahedron exceeds ~28%, i.e., $d_a/d_e > 1.28$. This result is in good agreement with the results of *ab initio* calculations where the effect of the CuO_6 octahedron elongation on the *d*-*d* transition spectra in CuO was studied.[63] When the d_a/d_e ratio increases further and exceeds ~1.36, the level $(3r^2 - z^2)$ becomes the highest.

Importantly, the position of the $(3r^2 - z^2)$ level, being a measure of the Jahn-Teller splitting, is often a matter of controversy. Since in the undistorted octahedron the states $(x^2 - y^2)$ and $(3r^2 - z^2)$ are degenerate, the splitting between these states in real copper compounds was often assumed to be small. For example, in literature one can find two different estimates for this splitting in $Sr_2CuO_2Cl_2$. A feature in the midinfrared absorption spectrum at 0.4 eV was assigned to the $(x^2 - y^2) \rightarrow (3r^2 - z^2)$ transition.[61] Later, based on the data of the RIXS spectra,[48] the energy of this transition was shifted higher to ~1.5 eV. First-principles calculations also gave a close value of 1.53 eV.[53] However, as this peak could not be directly resolved in experimental studies, the uncertainty about the position of the $(3r^2 - z^2)$ level remains. To the best of our knowledge, no experimental manifestations of the transition $(x^2 - y^2) \rightarrow (3r^2 - z^2)$ were found in other copper oxides, except for the present work.

Our simple approach predicts that in $Sr_2CuO_2Cl_2$ this level is indeed much higher that it was proposed.[61] Furthermore, we argue that this level has an energy of 2.065 eV and is the highest in the spectra of the Cu^{2+} ion in $Sr_2CuO_2Cl_2$, in contrast to estimates given in Refs. 48 and 53. Indeed, the elongation of the CuO_4Cl_2 octahedra is 44% and for such an elongation we can expect the level $(3r^2 - z^2)$ to be the highest. Moreover, Cl^{-} ions have a charge twice as low as oxygen ions in pure CuO_6 octahedra. Therefore, one can see the elongated CuO_4Cl_2 cluster as even stronger elongated CuO_6 octahedra, in which the Jahn-Teller should be large. We note that the validity of our estimate is supported by the energies obtained from our model for two other *d*-*d* transitions discussed above.

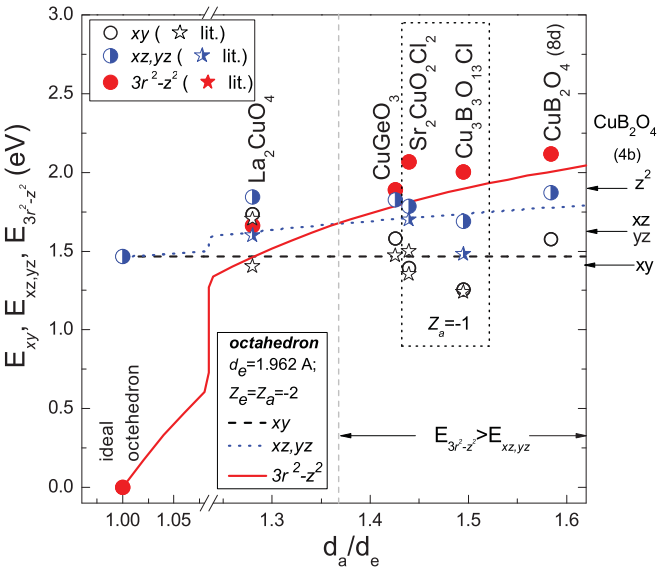

FIG. 7. (Color online) Dependence of the energies of the (xy) (open symbols), $(xz,\ yz)$ (half-open symbols), and $(3r^2 - z^2)$ (closed symbols) levels of Cu^{2+} ion on the elongation d_a/d_e of its octahedral coordination. Also shown by stars are the literature data (see Table V). Lines show the calculated dependence for these levels in the octahedron with the equatorial bond length $d_e = 1.962$ Å(averaged bond length in the considered copper compounds). On the right the corresponding energy levels are shown for the planar-square $4b$ Cu^{2+} position in CuB_2O_4. Vertical line separates the range of the octahedron elongations, where the level $(3r^2 - z^2)$ has the highest energy. Note, that the charge of the apical ligands in $Sr_2CuO_2Cl_2$ and $Cu_3B_7O_{13}Cl$ is $Z_{Cl} = -1$ instead of $Z_O = -2$ in other considered compounds.

Summarizing the results on the Jahn-Teller splitting in copper compounds obtained from our model, we can conclude that the $(x^2 - y^2)$-$(3r^2 - z^2)$ splitting in all considered materials is large. The level $(3r^2 - z^2)$ appears to be the highest among the $3d$ levels in the Cu^{2+} ion spectra in all compounds with the exception of La_2CuO_4 where the Cu-O equatorial bond length is $d_e = 1.8971$ Å.[30] In this respect, it is interesting to compare our estimates with the systematic theoretical *ab initio* study of this splitting.[63] In this work, midinfrared spectra of a number of the copper compounds including La_2CuO_4, $CuGeO_3$, and $Sr_2CuO_2Cl_2$ were calculated. Our estimates and the results of these calculations partly agree. This concerns the order of the $3d$ states of Cu^{2+} ion in La_2CuO_4 and $CuGeO_3$. The *ab initio* calculations for $Sr_2CuO_2Cl_2$ predict the $(3r^2 - z^2)$ state to be the lowest, which disagree with our estimates. We, however, argue that there is a systematic underestimation of the Jahn-Teller splitting in most of the *ab initio* calculations of the Cu^{2+} ion spectra known to date.

VIII. CONCLUSIONS

We presented and analyzed high-resolution α-, σ-, and π-polarized absorption spectra related to d-d electronic transitions in the copper metaborate CuB_2O_4 whose crystal symmetry is described by the tetragonal point group $\bar{4}2m$ and the space group $I\bar{4}2d$. In this structure, copper Cu^{2+} ions occupy two crystallographically distinct $4b$ and $8d$ positions. The absorption spectra in the 1.4–2.4 eV range are characterized by exceptionally rich fine structure. We succeeded to distinguish and identify six ZP lines responsible for the electronic transitions within the Cu^{2+} ions in both positions. The local symmetry of the Cu^{2+} ions in both positions was applied for constructing the energy-level scheme for the $(x^2 - y^2)$, (xy), $(xz,\ yz)$, and $(3r^2 - z^2)$ states. Symmetry analysis explains the polarization properties of ZP lines in $8d$ positions but only partly explains the polarization properties of the ZP lines in $4b$ positions. We suppose that the selection rules for transitions within the Cu^{2+} ions in the $4b$ positions are broken by magnetic ordering at $T_N = 21$ K and/or magnetic phase transitions at lower temperatures.

Reliable assignment of all six ZP lines to specific transitions allowed us to calculate genuine cubic Dq and tetragonal Ds and Dt crystal-field parameters for both positions of Cu^{2+} ions. By saying genuine we mean that the crystal-field parameters are calculated using the energy positions of narrow ZP lines but not the positions of the broad phonon-assisted bands usually observed in low-resolution optical or RIXS spectra. We show that the $(3r^2 - z^2)$ state is the highest $3d$ state in CuB_2O_4 for the both types of Cu^{2+} ion positions.

Using the obtained crystal-field parameters as the reference values and crystallographic data for Cu-O bond lengths, we estimated the values of Dq, Ds, and Dt parameters for several other cuprates. This allowed us to calculate the d-d transition energies in these materials. We note that here we used the point-charge model, which is usually very unreliable, when none of the values entering the model are known. However, the calculations presented here employ the genuine crystal-field parameters, which were precisely determined from the zero-phonon lines in the optical spectra of CuB_2O_4, as the reference values. Comparison of the calculated values and the data from the literature shows a remarkable agreement for all d-d transitions except for $(x^2 - y^2) \rightarrow (3r^2 - z^2)$. Thus our results allow us to conclude that the energy of this transition, which is a measure of the Jahn-Teller splitting, has been previously often underestimated.

ACKNOWLEDGMENTS

Useful discussions with W. Weber on crystal-field splitting of $3d$ states in cuprates are appreciated. We thank H.-J. Weber for the help in using Cary 2300 spectrophotometer. This work is supported by the Russian Foundation for Basic Research (project No. 09-02-00070) and Federal Agency for Science and Innovations (Grant No. 02.740.11.0384). A. M. K. acknowledges the financial support from the Committee for Science and Higher Education of the Government of Saint Petersburg.

[1] M. A. Kastner, R. J. Birgeneau, G. Shirane, and Y. Endoh, Rev. Mod. Phys. **70**, 897 (1998).

[2] D. N. Basov and T. Timusk, Rev. Mod. Phys. **77**, 721 (2005).

[3] Z. A. Kazei and I. B. Krynetskii, *Magnetic Properties of Non-Metallic Inorganic Compounds Based on Transition Elements: Perovskite-type Layered Cuprates (High Tc Superconductors and*

Related Compounds), edited by H. P. J. Wijn, Landolt-Börnstein, New Series, Vol. III/27f2 (Springer, Berlin, 1994) and Vol. III/27f2s (Springer, Berlin, 2002).

[4]D. I. Mendeleev, *Fundamentals of Chemistry* (St. Petersburg, 1909) (in Russian).

[5]M. Martinez-Ripoll, S. Martinez-Carrera, and S. Garcia-Blanco, Acta Cryst. B **27**, 677 (1971).

[6]G. K. Abdullaev and K. S. Mamedov, J. Struct. Chem. **22**, 637 (1981);[Zh. Strukt. Khim. 22, 184 (1981)].

[7]J. Schlueter, D. Pohl, and U. Golla Shindler, Neues Jahrbuch fuer Mineralogie-Abhandlungen **185**, 27 (2008).

[8]M. Boehm, B. Roessli, J. Schefer, A. S. Willis, B. Ouladdiaf, E. Lelièvre-Berna, U. Staub, and G. A. Petrakovskii, Phys. Rev. B **68**, 024405 (2003).

[9]B. Roessli, J. Schefer, G. Petrakovskii, B. Ouladdiaf, M. Boehm, U. Staub, A. Vorotinov, and L. Bezmaternikh, Phys. Rev. Lett. **86**, 1885 (2001).

[10]M. Boehm, B. Roessli, J. Schefer, A. Amato, C. Baines, U. Staub, and G. Petrakovskii, Physica B: Condens. Matter **318**, 277 (2002).

[11]A. I. Pankrats, G. A. Petrakovskii, M. A. Popov, K. A. Sablina, L. A. Prozorova, S. S. Sosin, H. Szimczak, R. Szimczak, and M. Baran, JETP Lett. **78**, 569 (2003).

[12]G. Nénert, L. N. Bezmaternykh, A. N. Vasiliev, and T. T. M. Palstra, Phys. Rev. B **76**, 144401 (2007).

[13]J. N. Hancock, G. Chabot-Couture, Y. Li, G. A. Petrakovskii, K. Ishii, I. Jarrige, J. Mizuki, T. P. Devereaux, and M. Greven, Phys. Rev. B **80**, 092509 (2009).

[14]K. S. Aleksandrov, B. P. Sorokin, D. A. Glushkov, L. N. Bezmaternykh, S. I. Burkov, and S. V. Belushchenko, Phys. Sol. State **45**, 42 (2003).

[15]Y. Kousuka, S. I. Yano, J. I. Kishine, Y. Yoshida, K. Inoue, K. Kikuchi, and J. Akimitsu, J. Phys. Soc. Jpn. **76**, 123709 (2007).

[16]M. A. Popov, G. A. Petrakovskii, and V. I. Zinenko, Phys. Solid State **46**, 491 (2004).

[17]S. N. Martynov, J. Exp. Theor. Phys. **109**, 979 (2009).

[18]Y. Yasuda, H. Nakamura, Y. Fujii, H. Kikuchi, M. Chiba, Y. Yamamoto, H. Hori, G. Petrakovskii, M. Popov, and L. Bezmaternikh, J. Phys. Condens. Matter **19**, 145277 (2007).

[19]M. Fiebig, I. Sänger, and R. V. Pisarev, J. Appl. Phys. **93**, 6960 (2003).

[20]S. Martynov, G. Petrakovskii, M. Boehm, B. Roessli, and J. Kulda, J. Magn. Magn. Mater. **299**, 75 (2006).

[21]R. V. Pisarev, I. Sänger, G. A. Petrakovskii, and M. Fiebig, Phys. Rev. Lett. **93**, 037204 (2004).

[22]M. Fiebig, V. V. Pavlov, and R. V. Pisarev, J. Opt. Soc. Amer. **22**, 96 (2005).

[23]M. Saito, K. Ishikawa, K. Taniguchi, and T. Arima, Phys. Rev. Lett. **101**, 117402 (2008).

[24]T. Arima, J. Phys. Condens. Matter **20**, 434211 (2008).

[25]S. W. Lovesey and U. Staub, J. Phys. Condens. Matter **21**, 142201 (2009).

[26]S. W. Lovesey and U. Staub, J. Phys. Condens. Matter **21**, 498002 (2009).

[27]A. B. P. Lever, *Inorganic Electronic Spectroscopy* (Elsevier, Amsterdam, 1984).

[28]R. R. Burns, *Mineralogical Applications of Crystal Field Theory*, 2nd ed. (Cambridge University Press, Cambridge, 1993).

[29]Th. Hahn, Editor, *International Tables for Crystallography: Space-group Symmetry*, 5th ed., Vol. A (Springer, 2005).

[30]M. Reehuis, C. Ulrich, K. Prokš, A. Gozar, G. Blumberg, S. Komiya, Y. Ando, P. Pattison, and B. Keimer, Phys. Rev. B **73**, 144513 (2006).

[31]M. Braden, G. Wilkendorf, J. Lorenzana, M. Aïn, G. J. McIntyre, M. Behruzi, G. Heger, G. Dhalenne, and A. Revcolevschi, Phys. Rev. B **54**, 1105 (1996).

[32]L. L. Miller, X. L. Wang, S. X. Wang, C. Stassis, D. C. Johnson, J. Faber Jr. and C.-K. Loong, Phys. Rev. B **41**, 1921 (1990).

[33]S. Sueno, J. R. Clark, J. J. Papike, and J. A. Konnert, Amer. Mineral. **58**, 691 (1973).

[34]H. Wilhelm, C. Cros, E. Reny, G. Damazeau, and M. Hanfland, J. Mater. Chem. **8**, 2729 (1998).

[35]D. S. McClure, Solid State Phys. **8**, 1 (1959).

[36]P. A. Markovin, A. M. Kalashnikova, R. V. Pisarev, and T. Rasing, JETP Lett. **86**, 712 (2007).

[37]A. S. Moskvin and R. V. Pisarev, Low Temp. Phys. **36**, 489 (2010).

[38]R. V. Pisarev, A. S. Moskvin, A. M. Kalashnikova, and T. Rasing, Phys. Rev. B **79**, 235128 (2009).

[39]W. Kleemann and Y. Farge, J. Phys. Lett. **35**, L135 (1974); J. Phys. **36**, 1293 (1975).

[40]J. Ferré, M. Regis, Y. Farge, and W. Kleemann, Physica B **89**, 181 (1977); J. Phys. C **12**, 2671 (1979).

[41]M. J. Riley, L. Dubicki, G. Moran, E. R. Krauzs, and I. Yamada, Inorg. Chem. **29**, 1614 (1990).

[42]J. Deisenhofer, I. Leonov, M. V. Eremin, C. Kant, P. Ghigna, F. Mayr, V. V. Iglamov, V. I. Anisimov, and D. van der Marel, Phys. Rev. Lett. **101**, 157406 (2008).

[43]M. Bassi, P. Camagni, R. Rolli, G. Samoggia, F. Parmigiani, G. Dhalenne, and A. Revcolevschi, Phys. Rev. B **54**, R11030 (1996).

[44]M. N. Popova, A. B. Sushkov, S. A. Golubchik, A. N. Vasiliev, and L. I. Leonyuk, J. Exp. Theor. Phys. **86**, 1227 (1996) [Zh. Eksp. Teor. Phys. **110**, 2230 (1996)].

[45]J. Zeman, G. Martinez, P. H. M. van Loosdrecht, G. Dhalenne, and A. Revcolevschi, Phys. Rev. Lett. **83**, 2648 (1999).

[46]N. N. Nesterova, R. V. Pisarev, and G. T. Andreeva, Phys. Status Solidi B **65**, 103 (1974).

[47]A. S. Moskvin, R. Neudert, M. Knupfer, J. Fink, and R. Hayn, Phys. Rev. B **65**, 180512 (2002).

[48]P. Kuiper, J.-H. Guo, C. Såthe, L.-C. Duda, J. Nordgren, J. J. M. Pothuizen, F. M. F. de Groot, and G. A. Sawatzky, Phys. Rev. Lett. **80**, 5204 (1998).

[49]D. Salamon, Ran Liu, M. V. Klein, M. A. Karlow, S. L. Cooper, S.-W. Cheong, W. C. Lee, and D. M. Ginsberg, Phys. Rev. B **51**, 6617 (1995).

[50]J. P. Falck, J. D. Perkins, A. Levy, M. A. Kastner, J. M. Graybeal, and R. J. Birgeneau, Phys. Rev. B **49**, 6246 (1994).

[51]G. Chabot-Couture, J. N. Hancock, P. K. Mang, D. M. Casa, T. Gog, and M. Greven, Phys. Rev. B **82**, 035113 (2010).

[52]R. V. Pisarev, V. V. Pavlov, A. M. Kalashnikova, and A. S. Moskvin, Phys. Rev. B **82**, 224502 (2010).

[53]D. S. Middlemiss, W. C. Mackrodt, J. Phys. Condens. Matter **20**, 015207 (2008).

[54]We note that according to M. Hidaka, T. Eguchi, and I. Yamada, J. Phys. Soc. Jpn. **67**, 2488, (1998), $KCuF_3$ has the space group symmetry $P2_12_12_1$ where the local symmetry of Cu^{2+} ions is 1. This symmetry makes allowed both ED and MD transitions between the 3*d* states in the crystal field. In Ref. 42, it was assumed that only MD transitions are allowed.

[55]G. F. Koster, J. O. Dimmock, R. G. Wheeler, and H. Statz, *Properties of The Thirty-two Point Groups* (MIT Press, Cambridge, Massachusetts, 1963).
[56]D. S. Ellis, J. P. Hill, S. Wakimoto, R. J. Birgeneau, D. Casa, T. Gog, and Y.-J. Kim, Phys. Rev. B **77**, 060501 (2008).
[57]A. K. McMahan, R. M. Martin, and S. Satpathy, Phys. Rev. B **38**, 6650 (1988).
[58]J. F. Annett, R. M. Martin, A. K. McMahan, and S. Satpathy, Phys. Rev. B **40**, 2620 (1989).
[59]R. L. Martin and P. J. Hay, J. Chem. Phys. **98**, 8680 (1993).
[60]W. Weber, Z. Phys. B **70**, 323 (1988).
[61]J. D. Perkins, J. M. Graybeal, M. A. Kastner, R. J. Birgeneau, J. P. Falck, and M. Greven, Phys. Rev. Lett. **71**, 1621 (1993).
[62]R. Liu, D. Salamon, M. V. Klein, S. L. Cooper, W. C. Lee, S.-W. Cheong, and D. M. Ginsberg, Phys. Rev. Lett. **71**, 3709 (1993).
[63]C. de Graaf and R. Broer, Phys. Rev. B **62**, 702 (2000).
[64]T. Ito, N. Morimoto, and R. Sadanaga, Acta Crystallogr. **4**, 310 (1951).